Pharmaceutical Research, Vol. 24, No. 9, September 2007 (© 2007)
DOI: 10.1007/s11095-007-9298-0

Research Paper

Effects of Carrier on Disposition and Antitumor Activity of Intraperitoneal Paclitaxel

Max Tsai,[1,3] Ze Lu,[1,2] Jie Wang,[1,2] Teng-Kuang Yeh,[1,2,4] M. Guillaume Wientjes,[1] and Jessie L.-S. Au[1,5]

Received December 25, 2006; accepted March 15, 2007; published online April 20, 2007

Purpose. The rationale for intraperitoneal (IP) chemotherapy is to expose peritoneal tumors to high drug concentrations. While multiple phase III trials have established the significant survival advantage by adding IP therapy to intravenous therapy in optimally debulked ovarian cancer patients, the use of IP chemotherapy is limited by the complications associated with indwelling catheters and by the local chemotherapy-related toxicity. The present study evaluated the effects of drug carrier on the disposition and efficacy of IP paclitaxel, for identifying strategies for further development of IP treatment.
Materials and Methods. Three paclitaxel formulations, i.e., Cremophor micelles, Cremophor-free paclitaxel-loaded gelatin nanoparticles and polymeric microparticles, were evaluated for peritoneal targeting advantage and antitumor activity in mice after IP injection. Whole body autoradiography and scanning electron microscopy were used to visualize the spatial drug distribution in tissues. A kinetic model, depicting the multiple processes involved in the peritoneal-to-plasma transfer of paclitaxel and its carriers, was established to determine the mechanisms by which a drug carrier alters the peritoneal targeting advantage.
Results. Autoradiographic results indicated that IP injection yielded much higher paclitaxel concentrations in intestinal tissues relative to intravenous injection. Compared to the Cremophor and nanoparticle formulations, the microparticles showed slower drug clearance from the peritoneal cavity, slower absorption into the systemic circulation, longer residence time, 10- to 45-times greater peritoneal targeting advantage and ~2-times longer increase in survival time ($p<0.01$ for all parameters).
Conclusions. Our results indicate the important roles of drug carrier in determining the peritoneal targeting advantage and antitumor activity of IP treatment.

KEY WORDS: carrier; intraperitoneal therapy; microparticles; paclitaxel.

INTRODUCTION

The rationale for intraperitoneal (IP) chemotherapy is to expose tumors located in the peritoneal cavity to high drug concentrations based on spatial proximity. IP therapy has been safely administered to cancer patients and provides 20- to 1,000-fold higher peritoneal concentrations compared to plasma concentrations for cisplatin, 5-fluorouracil, doxorubicin, and paclitaxel (1–3).

Several clinical studies have demonstrated the activity of IP paclitaxel and cisplatin against advanced ovarian cancer (4–11). The results of six randomized trials show that IP therapy yielded, on average, a 21.6% decrease in the risk of death and 12-month longer overall survival time (12). The 16-month survival extension by adding IP chemotherapy to intravenous chemotherapy, shown in the most recently completed phase III trial by the Gynecological Oncology Group (GOG-172), is considered the most significant advance in ovarian cancer research in the last 15 years (12,13).

The earlier clinical trials of IP paclitaxel were conducted using the first formulation approved by the U.S. Food and Drug Administration, where paclitaxel is solubilized in 50:50 Cremophor EL:ethanol (e.g., Taxol®, referred to as Cremophor formulation). In humans, IP paclitaxel/Cremophor is slowly cleared from the peritoneal cavity, with a 28-times longer elimination half-life compared to 5-fluorouracil, cisplatin or doxorubicin (>72 h vs 1–3 h) (2,14,15). A more recent study evaluated the role of Cremophor on the clearance of paclitaxel in four patients given an IP dose of radiolabeled paclitaxel in tracer quantity on day 1 followed by an IP dose of the Cremophor formulation on day 4 (16). The two formulations showed different dispositions. The

[1] College of Pharmacy, The Ohio State University, Columbus, Ohio, USA.
[2] Optimum Therapeutics, LLC, Columbus, Ohio, USA.
[3] *Present address:* Schering Plough, Kenilworth, New Jersey, USA
[4] *Present address:* National Health Research Institute, Taipei, Taiwan
[5] To whom correspondence should be addressed. (e-mail: au.1@osu.edu

ABBREVIATIONS: AUC, area under curve; AUMC, area under moment curve; HPLC, high pressure liquid chromatography; IP, intraperitoneal; MRT, mean residence time; MST, median survival time; PBS, phosphate-buffered saline; PLG, poly(D,L-lactide-co-glycolide); SEM, scanning electron microscope.

radiolabeled dose showed a significantly higher absorption into the systemic circulation (100 vs 31%) and a shorter residence time in peritoneal fluid (7 vs 41 h). Another study evaluated the role of formulation on the peritoneal targeting advantage of paclitaxel and docetaxel in rats. The results showed no difference in absorption rate constant in the peritoneal absorption when both taxanes were formulated in Cremophor whereas 20-times more rapid and more extensive absorption was observed for docetaxel formulated in Tween-80 (17). These differences in pharmacokinetics led to the conclusion that the entrapment of paclitaxel in Cremophor micelles extends the residence time in the peritoneal cavity. However, because the entrapment of paclitaxel in Cremophor micelles reduces the free drug fraction available to tumors (18), it is uncertain whether a longer residence of the Cremophor formulation translates to greater antitumor activity.

Extensive efforts have been invested in developing alternative formulations of paclitaxel for intravenous administration, in part to overcome the hypersensitivity associated with Cremophor. In 2005, FDA approved a second formulation where paclitaxel is conjugated to albumin (Abraxane®), based on its superior activity in breast cancer patients who had received prior chemotherapy. The higher activity of Abraxane® may be due to preferential distribution to tumors (19–21). Our laboratory and others have shown that the tissue distribution of paclitaxel, when given intravenously, is highly dependent on the carrier (22,23). Abraxane® has not been evaluated in IP therapy.

In spite of the demonstrated survival advantage, the use of IP chemotherapy is limited by several complications, i.e., infection due to prolonged use of indwelling catheter and local toxicity (e.g., abdominal pain, intestinal toxicity). These problems led to the inability of a majority of patients (up to nearly 60%) to complete the scheduled six treatment cycles (5,9) and the reluctance of the medical community to use IP therapy (13).

One approach to overcome the catheter-related complications is to use sustained release drug formulations that require less frequent dosing. Early research efforts in this area have shown promising results. For example, IP administration of cisplatin encapsulated in poly(lactic acid) microparticles (100–200 μm diameter, releasing cisplatin over 4 weeks) to mice resulted in localization of microparticles and significantly higher drug concentrations in tumors located on the omentum, compared to cisplatin solution (24). Likewise, IP administration of poly(lactide-co-glycolide) microparticles that release 5-fluorouracil over 3 weeks to mice yielded significantly higher drug concentrations in IP tissues (omentum, mesentery) compared to systemic tissues (blood, lungs, heart) (25). A recent phase I trial of IP administration of Paclimer®, a biodegradable polymer microsphere formulation containing 10% w/w paclitaxel (53 μm diameter) in ovarian cancer patients indicated good tolerability of microparticles but also revealed foreign body reactions and residue polymer filaments in abdominal tissues seven months after treatment (26).

The present study evaluated the effects of carrier on the disposition and efficacy of IP paclitaxel. We evaluated three paclitaxel formulations with different particle size and release rate, i.e., Cremophor formulation, Cremophor-free paclitaxel-loaded gelatin nanoparticles and Cremophor-free paclitaxel-loaded polymeric microparticles.

MATERIALS AND METHODS

Chemicals and Reagents

Paclitaxel was purchased from Handetech (Houston, TX). Cephalomannine was obtained from the National Cancer Institute (Bethesda, MD), and 3″-^{3}H-paclitaxel (specific activity, 10.6 Ci/mmol) from the National Cancer Institute or Moravek Biochemicals (Brea, CA). High performance liquid chromatographic (HPLC) analysis showed that paclitaxel, 3″-^{3}H-paclitaxel, and cephalomannine were >99% pure. Poly(D,L-lactide-co-glycolide) 50:50 (PLG, intrinsic viscosity of 0.18 dl/g) was purchased from Birmingham Polymers (Birmingham, AL), cefotaxime sodium from Hoechst-Roussel (Somerville, NJ), gentamicin from Solo Park (Franklin Park, IL), and McCoy's culture medium from Life Technologies (Grand Island, NY). Poly(vinyl alcohol) or PVA, Type A gelatin from porcine skin, Tween-20, sodium sulfate, sodium metabisulfite, pronase, Cremophor EL and glutaraldehyde (25% in water) were purchased from Sigma Chemical (St. Louis, MO). HPLC solvents were purchased from Fisher Scientific (Fair Lawn, NJ). All chemicals and reagents were used as received.

Overview of Experiments

Two groups of studies were performed. The first group was to visualize the spatial distribution of paclitaxel in the whole body and was investigated using autoradiography of ^{3}H-paclitaxel. The second group evaluated the effects of carrier on (a) clearance of paclitaxel from the peritoneal cavity, (b) apparent rate and extent of absorption from the peritoneal cavity, and (c) antitumor activity. These latter studies required blood and peritoneal fluid samples and were conducted using nonradiolabeled drug and HPLC analysis of drug concentrations. All studies used the same dose of paclitaxel (equivalent to 10 mg/kg), to ensure that the data was not affected by the nonlinear pharmacokinetics of paclitaxel (27,28).

Preparation of Paclitaxel Formulations

Three formulations were studied. For the Cremophor formulation, paclitaxel was dissolved in Cremophor EL:ethanol (1:1, v:v) and then diluted with sterile physiological saline to a final concentration of 1 mg/ml.

Paclitaxel-loaded gelatin nanoparticles were prepared as previously described (29). Briefly, to a 2% gelatin solution (800 mg in 40 ml water containing of 2% Tween 20) heated to 40°C, 8 ml of a 20% aqueous solution of sodium sulfate and then 4 ml of isopropanol containing 8 mg of paclitaxel were added. Additional sodium sulfate solution (about 26 ml) was added until the solution turned turbid due to formation of gelatin aggregates. Approximately 4 m of distilled water was then added to obtain a clear solution. Glutaraldehyde (25% in water, 1.6 ml) was added to cross-link the gelatin

molecules, and 10 min later, sodium metabisulfite solution (12% in water, 20 m) to stop the cross-linking process. The crude product was purified on a large Sephadex G-50 column (100 cm length×4.8 cm I.D.). The nanoparticle fraction was lyophilized in a Freezone 4.5 lyophilizer (Labconco Corporation; Kansas City, MO).

For the microparticles, PLG (190 mg) and paclitaxel (10 mg) were co-dissolved in 5 ml of methylene chloride, and emulsified in 20 ml of 1% PVA aqueous solution by homogenization for 30 s. The emulsion was mixed with 500 ml of 0.1% PVA, and stirred at 1,000 rpm at room temperature and ambient pressure to evaporate the methylene chloride. Microparticles pellet was collected by centrifugation, washed three times with deionized water to remove residual PVA, lyophilized, and stored at 4°C.

Characterization of Paclitaxel-loaded Nanoparticles and Microparticles

The diameter of particles was determined using scanning electron microscopy (SEM). Briefly, paclitaxel-loaded gelatin nanoparticles or PLG microparticles were suspended in distilled water. The mixture was added drop-wise onto metal foil and allowed to air-dry. The dried microparticles were coated with gold-palladium for 80 s under an argon atmosphere. The size and surface morphology of the nanoparticles and microparticles were examined using a Phillips XL 30 scanning electron microscope. Digital images were recorded and analyzed using Optimas imaging software v. 6.5 (Media Cybernetics). At least 300 particles were measured. Volume mean diameter (Dv) and number mean diameter (Dn) were determined, respectively. Polydispersity index (PDI), a measurement of distribution, was calculated as $(D_{90\%}—D_{10\%})/D_{50\%}$, where $D_{90\%}$, $D_{50\%}$ and $D_{10\%}$ were the respective volume diameters at 90, 50, and 10% cumulative volumes.

To determine drug loading, nanoparticles (2 mg) were dispersed in 0.5 ml of PBS and digested with 0.5 ml of Pronase (1 mg/ml in PBS) in a metabolic shaker at 37°C for about 1 h (or when a clear solution was obtained). Microparticles (3 mg) were dissolved in 1 ml methylene chloride. Aliquots of these solutions were extracted and processed for HPLC analysis. The reference standard samples consisted of mixtures of blank gelatin nanoparticles or blank PLG microparticles and known amounts of paclitaxel.

For *in vitro* drug release, gelatin nanoparticles were incubated in PBS (2 mg in 50 ml) and PLG microparticles in PBS containing 0.1% of Tween 80 (2.5 mg in 10 ml), pH 7.4, at 37°C. After withdrawing samples for analysis, equal volumes of fresh release medium were added to maintain a sink condition.

Animal Protocols

Female nude Balb/C mice (6–8 weeks old, 16–18 g body weight) were obtained from NCI/Charles River Laboratories, and housed and cared for in accordance with institutional guidelines. Mice were allowed at least 3 days to acclimate to the surroundings and had access to food and water *ad libitum*. Dosing solutions were administered between 8 A.M. and 12 noon. Intravenous administration was through a tail vein. IP administration was through an angiocatheter (18-gauge, 1.3 mm; Becton-Dickinson; Sandy, UT) inserted into the peritoneal cavity. At predetermined times, mice were anethesized and blood samples were collected through the retro-orbital venous plexus. Afterward, 2 ml of physiologic saline was instilled in the peritoneal cavity through an indwelling angiocatheter and withdrawn after gently massaging the abdomen for 2–5 min. The washing procedures were repeated and the two lavage samples were pooled. All samples, dosing solutions, and remaining animal carcasses were stored at −70°C until analysis.

Whole-body Autoradiography

We used whole body autoradiography to study the spatial distribution of paclitaxel in peritoneal and systemic tissues, in mice given an IP or intravenous dose of the Cremophor formulation (containing 10 mg/kg non-radiolabeled paclitaxel plus 1 mCi/kg ^{3}H-paclitaxel). At predetermined times, an animal processed for whole body autoradiography as described by Ullberg (30), with the following minor modifications. Immediately after euthanasia, an animal was placed in hexane cooled in dry ice. The frozen carcasses were embedded in a carboxymethyl cellulose gel (Bondex International Inc., St. Louis, MO). The gel molds were immersed in dry ice/hexane mixture at −70°C for 20 min and stored at −20°C until sectioning. Frozen whole animal coronal sections of 30–40 μm were obtained using a PMV 450 cryomicrotome (Stockholm, Sweden), kept frozen at −25°C and mounted on Scotch tape 800 (3M Co., St. Paul, MN). Multiple sections were taken from various planes, allowing for complete examination of all major organs. Sections were lyophilized at −25°C for up to 3 days. Photographs of the dried sections were taken using a 35 mm camera (Nikon N50) and Kodak Ektachrome 100 color film (Kodak Inc., Rochester, NY). For standards, we used two commercially available, pre-calibrated tritium microscale autoradiography strips, each containing eight different levels of radioactivity (RPA506 containing 109.4, 66.7, 40.2, 33.5, 23.6, 8.7, 4.7, 3.0 μCi/g, RPA507 containing 15.9, 7.84, 4.87, 2.01, 1.00, 0.48, 0.26, 0.10 μCi/g; Amersham Corporation, Arlington Heights, IL). The reference strips and tissue sections were placed together against tritium-sensitive film (Hyperfilm tritium autoradiography film; Amersham, Arlington Heights, IL) and exposed for 7 days at 4°C. After exposure, the autoradiography films were processed for film development. The film was moved through the following processing tanks in succession at room temperature: (a) developer tank (Kodak D-19) for 5 min, (b) stop tank (Kodak Indicator Stop Solution; 16 ml per liter) for 30 s, (c) acid-hardening fixing bath (Kodak F-5) for 5 min, (d) washing tank (deionized water) for 5 min, and (e) rinsing tank (Kodak Photo-Flo 200 Solution; 5.5 ml per 1.10 liter) for 30 s, and then air-dried. A digitized image was captured using a scanner (MicroTek ScanMaker V310), and analyzed using the NIH ImageJ software (http://rsb.info.nih.gov/nih-image/download.html). The densitometry measurements of the reference strips were used to generate a standard curve. Tissues-of-interest in each tape section were then selected, digitized, and converted to relative concentrations using the standard curve.

Scanning Electron Microscopy of Particle Distribution on Diaphragm

Mice were given an IP injection of paclitaxel-loaded gelatin nanoparticles or microparticles (n=3 per formulation). After 15 min, mice were euthanized and their diaphragms were excised, fixed in PBS containing 4% glutaldehyde for 2 h, lyophilized, coated with gold gold-palladium and observed under SEM (Philips XL 30 SEM). Images were further analyzed using NIH ImageJ software to obtain the lengths and widths of lymphatic duct openings on diaphragm surface.

HPLC Analysis

Extraction of paclitaxel from aqueous samples including plasma and peritoneal lavage samples, and samples obtained from the drug loading/release experiments using ethyl acetate and the column-switching HPLC assay (31) was as previously described (31). The methylene chloride solution of PLG microparticles was analyzed without extraction. Cephalomannine was used as the internal standard. The HPLC stationary phase consisted of a cleanup column (Nova-Pak C_8, 4 μm particle, 3.9 mm×75 mm) from Waters (Mildford, MA) and an analytical column (Bakerfield C_{18}, 5 μm particle, 4.6 mm×250 mm) obtained from Mallinkrodt Baker (Phillipsburg, NJ). Samples were injected into the cleanup column and eluted with a mobile phase consisting of 37.5% acetonitrile at a rate of 1.0 ml/min. The analytical mobile phase consisting of 49% acetonitrile was directed through the analytical column at a flow rate of 1.2 ml/min. The UV detector was set at 229 nm and its limit of detection for paclitaxel was 1 ng per injection.

Pharmacokinetic Data Analysis

The effects of carrier on paclitaxel absorption from the peritoneal cavity were studied by comparing the rate and extent of absorption into the systemic circulation. The systemic bioavailability of an IP dose of each of the three formulations was calculated using the pharmacokinetics of an intravenous dose of the Cremophor formulation as the reference. We did not use intravenous nanoparticles as references because the particles were not expected to reflect the drug entity absorbed from the peritoneal cavity (i.e., free drug). The area under concentration/dose-time curve (AUC) and the area under moment curve (AUMC) were calculated using the trapezoid rule. The mean residence time (MRT) was calculated as AUMC/AUC. Apparent peritoneal absorption rate constant was calculated from the initial slope of the log-linear plot of percent of dose-time curve. Peritoneal targeting advantage was calculated as ratios of AUC in peritoneal cavity from 0 to 168 h to AUC in plasma from 0 to 24 h.

Antitumor Activity

The effects of carrier on the survival benefits of paclitaxel formulations were investigated. The human xenograft tumor model should satisfy several criteria, i.e., 100% take rate (tumor development in all animals after IP implantation of tumor cells), reproducible and relatively rapid disease establishment and progression. We evaluated two cell lines, human pancreatic Hs766T cancer cells (gift from Dr. Byoungwoo Ryu, John Hopkins Medical Institute, Baltimore, MD) and human ovarian SKOV3 cells (American Type Culture Collection, Manassas, VA), and successfully developed an IP Hs766T model that satisfied the above criteria.

Hs766T cells were maintained in Dulbecco's modified Eagle's media containing 9% fetal bovine serum, 2 mM L-glutamine, 90 μg/ml gentamicin, and 90 μg/ml cefotaxime sodium at 37°C in a humidified atmosphere of 5% CO_2 in air. IP implantation of the original cell line into female athymic nu/nu mice (20×10^6 cells in a volume of 0.5 ml) resulted in a take-rate of 30–40% (tumors were evident after 2 weeks). Reimplantation of cells harvested from the ascites fluid in animals with established IP tumors (expanded in culture) into new recipient hosts resulted in a 100% take-rate; all animals died within 40 days (n=12, median survival time or MST of 21.5 days). Drug treatment was initiated at about 50% of MST of the control group (i.e., day 10 after tumor implantation). Animals received physiological saline, paclitaxel-loaded Cremophor micelles, nanoparticles, or microparticles (paclitaxel-equivalent dose of 40 mg/kg for all three formulations).

Post-mortem autopsies were performed to evaluate the cause of death. Typically, deaths that occurred within 10 days post-treatment were considered treatment-related deaths (e.g., >15% body weight loss, internal hemorrhage due to faulty injections). Deaths that occurred at later times and accompanied by tumor nodules and/or tumor infiltration into organs were considered deaths due to disease progression.

Statistical Analysis

MST and increase in MST were determined. The levels of significance in the differences in survival times were analyzed using the log-rank test. Differences in peritoneal clearance and systemic absorption between the microparticle and other groups were analyzed using one-way ANOVA with Tukey post test. Statistical analysis was performed using SAS (Cary, NC). P values of less than 5% were considered statistically significant.

RESULTS

Spatial Distribution of ^{3}H-paclitaxel after Intraperitoneal and Intravenous Injection

This was studied using the Cremophor formulation. Figure 1a shows a whole body section of a mouse. Figure 1b shows the images obtained using the microscale tritium reference strips. Figure 1c and d show the autoradiographs of animals obtained at different time points after intravenous and IP treatments. Figure 1e shows the concentration-time profiles obtained from densitometric analysis of the autoradiographs; the data represented the relative concentrations and not the absolute concentrations because we were not able to get the actual weight of the tissue on the tape sections. Further, as autoradiographs detected total radioactivity and did not distinguish the unchanged paclitaxel from its metabolites, the concentrations represented total drug concentrations.

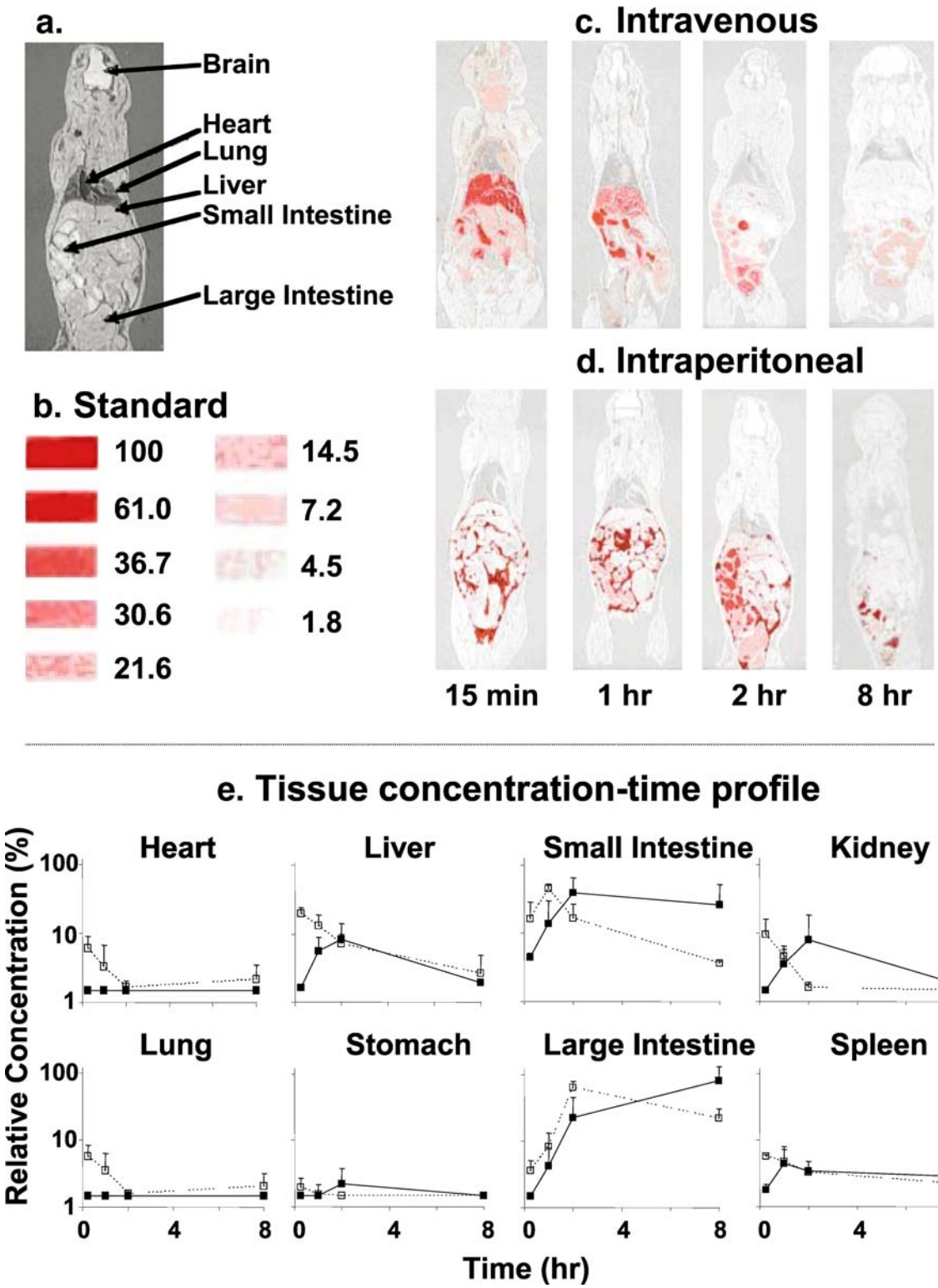

Fig. 1. Spatial and tissue distribution of intravenous and IP injections of ^{3}H-paclitaxel solubilized in Cremophor EL/ethanol. A mouse was given an IP or IV injection of the Cremophor formulation of paclitaxel (a mixture of radiolabeled and nonlabeled paclitaxel, equivalent to 10 mg/kg and 1 mCi/kg). **a** Whole body section of a mouse. **b** Densitometric signals of microscale tritium standards. The numbers correspond to the relative concentrations, with the highest level set at 100%. **c** Whole body autoradiographs at various time points after an intravenous dose. **d** Whole body autoradiographs after an IP dose. No radioactivity was detected in the brain following either administration route (limit of detection was 2.01 μCi/g corresponding to 1.8% relative level). **e** Relative tissue concentration-time profiles, determined by digital videodensitometry, after an intravenous (*open symbols*, *dotted lines*) or IP (*closed symbols*, *solid lines*) dose. No radioactivity was detected in the brain following either administration route. At least three mice were used for each time point. Mean ± S.D.

Table I. Effects of Carrier on Peritoneal Clearance and Systemic Absorption of IP Chemotherapy

Carrier	Drug Loading (n=3) (%)	Particle Size and Size Distribution Dv (μm), Dn (μm), PDI	Drug Release *in vitro*	Peritoneal Cavity			Plasma						Peritoneal Targeting Advantage
				% of Dose Remaining at 24 h	AUC from 0 to 168 h (% of dose*h)	Peritoneal Absorption Rate Constant (h^{-1})	MRT (h)	T_{max} (h)	C_{max} (μg/ml)	AUC from 0 to 24 h (μg*h/ml)	F (%)	MRT (h)	
Nanoparticle	0.47±0.07	0.90, 0.59, 0.81	Complete release in 4 h	0.01±0.01	46.7	0.39	1.0	0.5	1.00±0.55	6.39	37.7	8.7	7.31
Cremophor	–	0.013, –, –	~10% at steady state *	0.06±0.02	179	0.16	2.8	1	0.85±0.19	6.15	36.3	7.2	29.1
Microparticle	3.77±0.26	5.73, 3.63, 0.78	70% in 24 h	7.14±2.62**	559	0.10	28.5	1	0.17±0.04**	1.65	9.7	14.9	339

Areas under dose/concentration-time curves (AUC) and areas under moment curves (AUMC) were calculated using the trapezoid rule. The mean residence time (MRT) was calculated as AUMC/AUC. Apparent peritoneal absorption rate constant was calculated from the initial slope of the log-linear plot of % dose versus time curve. T_{max} is the time when the maximal plasma concentration (C_{max}) was observed. The systemic bioavailability F was calculated as the ratio of (plasma AUC after IP paclitaxel) to (AUC of intravenous Cremophor paclitaxel, which equaled 169 μg*h/ml). Peritoneal targeting advantage was calculated as ratio of (AUC in peritoneal cavity from 0 to 168 h) to (AUC in plasma from 0 to 24 h). At least three mice were used for each time point. Mean ± S.D.
*Because drug release from the Cremophor micelles is controlled by partition, the data for this formulation represents the free fraction at steady state (32).
**p<0.01 compared to other groups (one-way ANOVA with Tukey post test).

After an intravenous dose, the highly perfused systemic tissues showed the highest concentrations at early time points, as would be expected. For example, after 15 min, most of the radioactivity resided in the liver, followed by the small intestine, kidney, heart, lung, spleen, and colon. The subsequent decrease in the radioactivity in the liver coincided with the increase in the lumen of the small intestine (e.g., 1 h), indicating a liver-to-intestine drug transfer. Similarly, a surge in radioactivity in the lumen of the large intestine at 2 h coincided with a decrease in the small intestine, indicating the movement of radioactivity from the small intestine to the large intestine. Within 2 h, radioactivity in most organs and tissues, except the small and large intestines, had decreased to levels close to or indistinguishable from the background signal.

After IP administration, nearly all of the radioactivity was confined to tissues and organs in the peritoneal cavity at all times. At 15 min, the radioactivity was located primarily in the space surrounding the visceral tissues, indicating that the drug remained in the dosing solution. The intestinal tissues showed the highest radioactivity, followed by the liver, kidney

Fig. 2. Particle size distribution and *in vitro* drug release of paclitaxel-loaded gelatin nanoparticles and PLG microparticles. **a** Particle size distribution. *Blank bar*: paclitaxel-loaded gelatin nanoparticles (mean number diameter Dn was 0.59 μm, mean volume diameter Dv was 0.90 μm, and polydispersity index PDI was 0.81); *filled bar*: paclitaxel-loaded PLG microparticles (Dn was 3.63 μm, Dv was 5.77 μm, PDI was 0.78). **b** *in vitro* drug release in PBS at 37°C under sink conditions. (*filled circle*), paclitaxel-loaded gelatin nanoparticles; (*filled square*), paclitaxel-loaded PLG microparticles, Mean ± S.D., n=3.

and spleen, whereas the levels in the heart and lung were nearly indistinguishable from background.

Characterization of Paclitaxel-loaded Gelatin Nanoparticles and PLG Microparticles

Table I summarizes the drug loading in paclitaxel-loaded gelatin nanoparticles and PLG microparticles. Figure 2a shows the size distribution of paclitaxel-loaded gelatin nanoparticles and PLG microparticles; the respective mean number diameter and mean volume diameter were 0.59 and 0.90 μm (with total of 431 nanoparticles counted), and 3.63 and 5.77 μm (with total of 340 microparticles counted), and the respective polydispersity indices were 0.81 and 0.78. Figure 2b shows the drug release profiles; the nanoparticles showed a more rapid and complete release (100% in 4 h) compared to the microparticles (70% in 24 h).

Effects of Carrier on Paclitaxel Clearance from Peritoneal Cavity and Absorption into Systemic Circulation

The disposition of a drug administered by IP injection in the form of a carrier consists of multiple kinetic processes, i.e., drug release from carrier, clearance from the peritoneal cavity, absorption from the peritoneal cavity to the systemic circulation (e.g., plasma), and elimination (first pass and systemic). As shown below, many of these processes are affected by the drug carrier.

Figure 3a depicts a model describing the kinetic processes involved in drug disposition in the peritoneal cavity and

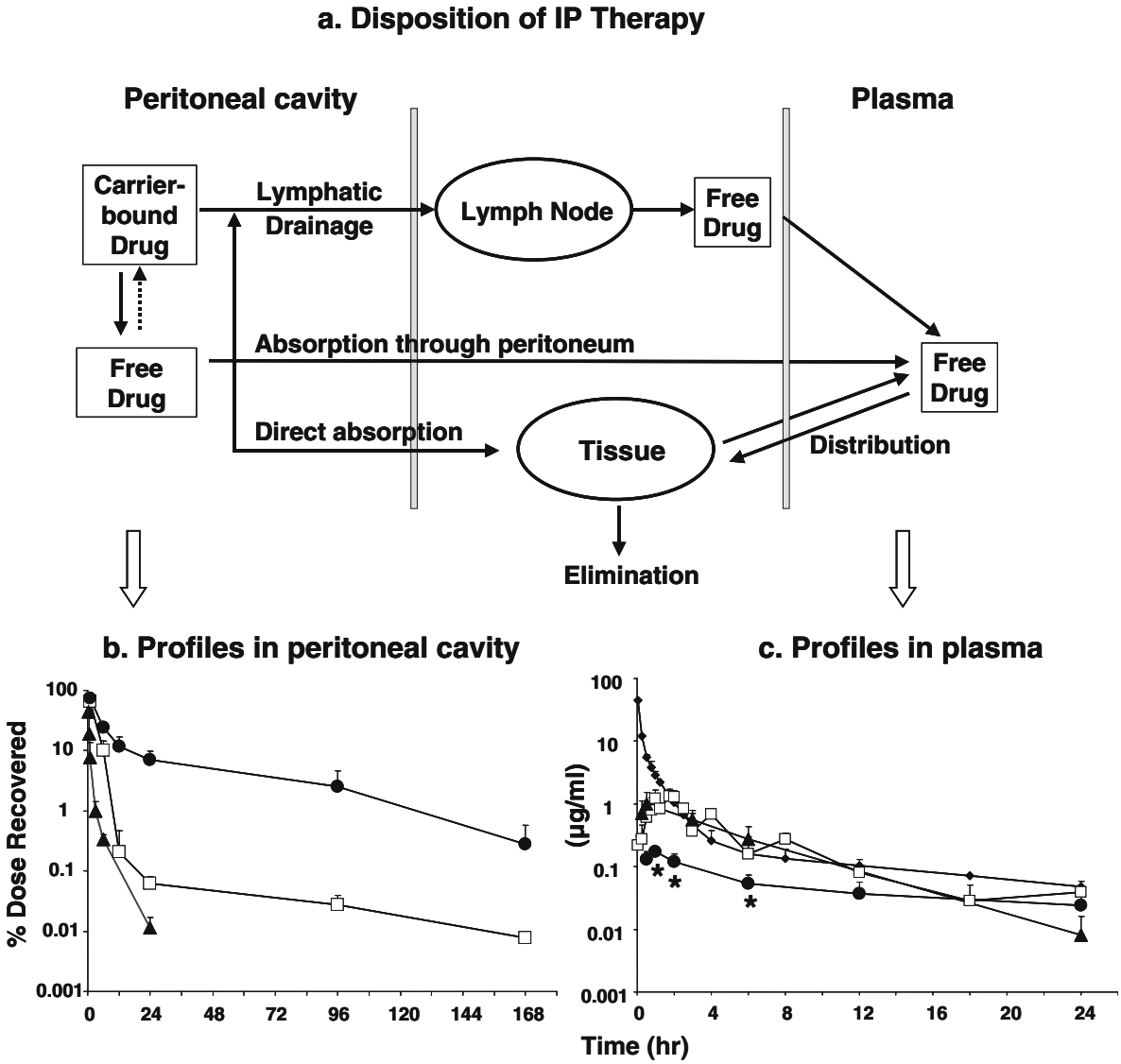

Fig. 3. Effects of carrier on disposition of an IP dose of paclitaxel. Three formulations, i.e., paclitaxel solubilized in Cremophor EL/ethanol (*empty square*), paclitaxel-loaded gelatin nanoparticles (*filled triangle*), and paclitaxel-loaded polymeric microparticles (*filled circle*) were administered by IP injections at 10 mg/kg. For comparison, an additional group of mice received an intravenous dose of paclitaxel solubilized in Cremophor EL/ethanol (♦). **a** A model of kinetic processes during IP treatment. Paclitaxel concentration-time profiles in plasma (**b**) and peritoneal lavage samples (**c**). Note the different time scales for panels **b** and **c**. At least three mice were used for each time point. Mean ± S.D. *, $p<0.001$, compared to other groups by one-way ANOVA with Tukey post test.

systemic circulation after an IP administration of drug-loaded carriers. Based on the nature of the drug release, we proposed two separate kinetic processes for the three formulations. For the nanoparticles and microparticles, paclitaxel was incorporated into the particles through chemical manipulations and would not re-enter the particles after release. For the Cremophor formulation, paclitaxel would be able to partition in and out of the micelles. Micelles are formed at Cremophor concentration above 0.01%; the free fraction of paclitaxel decreased from 100% in the absence of Cremophor to 23 and 11%, respectively, in 0.25 and 1% Cremophor (32). The initial Cremophor concentration in the dosing solution was 2.5% or above the threshold for forming micelles. The concentration during the duration of IP therapy, due to the absorption/removal of water from the cavity, would remain above this threshold. Hence, the model included a step for paclitaxel to re-enter the Cremophor micelles.

The model included two major mechanisms of clearance from the peritoneal cavity and entry into the systemic circulation, i.e., absorption through the peritoneum and drainage through the lymphatic ducts. For transport across the peritoneum, there are no known active processes; absorption (by diffusion or convection) through the peritoneum, a thin membrane (75 and 90 μm thick in rats and man, ref. (33), is a major path for small compounds with molecular weight of less than 20 kD (34). Larger compounds or particulates are drained through the lymphatic ducts (35,36). Similar clearance was observed for particulates at a size range between 50 to 700 nm (36). Within the lymphatic system, smaller particulates (<50 nm) can pass through lymph nodes while larger particulates (>500 nm) are mostly trapped in lymph nodes (36). Hence, the model assumed that only the free drug was absorbed into the systemic circulation, whereas the drug concentrations in the peritoneal lavage samples represented the sum of free drug and carrier-entrapped drug. The model also incorporated the drug distribution into peritoneal organ and tissue by direct penetration, and the distribution into the first-pass organs including liver and intestines.

Figure 3b shows the kinetics of paclitaxel in the peritoneal fluid, and Table I summarizes the results. Because the residual drug in the peritoneal cavity was recovered by washing the cavity, only the total drug amounts in the lavage samples (instead of actual drug concentrations in the peritoneal fluid) could be accurately determined. Furthermore, the drug levels, determined using HPLC, represented the total drug comprising of free and carrier-bound drug. The clearance of the paclitaxel delivered in Cremophor and nanoparticle formulations was rapid, resulting in <0.1% of the dose remaining after 24 h. In comparison, the clearance of the microparticle formulation was slower with a 40–75% lower apparent elimination rate constant, resulting in 17–700 times higher residual peritoneal concentrations at 24 h, 10–28 times longer mean residence time in the peritoneal cavity, and 3–12 times higher total exposure.

Effects of Carrier on Paclitaxel Absorption into Systemic Circulation and Peritoneal Targeting Advantage

Figure 3c shows the plasma paclitaxel concentration-time-profiles resulting from IP administration of the three formulations. Also shown are the results obtained from an intravenous dose of the Cremophor formulation; the calculated clearance of the total paclitaxel concentrations (sum of free and Cremophor micelles-entrapped drug) was 0.59 l/h/kg. Note that this value represents the apparent clearance and not necessarily the true clearance of free paclitaxel. Table I summarizes the pertinent pharmacokinetic parameters.

The profiles for all three formulations, administered by IP injection, showed increasing plasma concentrations at early time points followed by a decline. This kinetic behavior is typical for absorption from an extravascular site. The Cremophor and nanoparticle formulations showed nearly superimposable profiles and pharmacokinetic parameters. In comparison, the microparticle formulation showed ~5-times lower peak plasma concentration and AUC over 24 h. Plasma concentrations were below the detection limit after 24 h for all three formulations.

Compared to intravenous administration of the same dose, IP administration of the Cremophor and nanoparticle formulations yielded 2 to 200-fold lower plasma concentrations at the early time points (up to 1 h), followed by comparable concentrations at later time points.

Table I shows the peritoneal targeting advantage, for the three formulations. The rank order was microparticles > Cremophor formulation > nanoparticles, with respective ratios of about 340, 30 and 7. It is noted that these values represented the total of free and carrier-entrapped drugs.

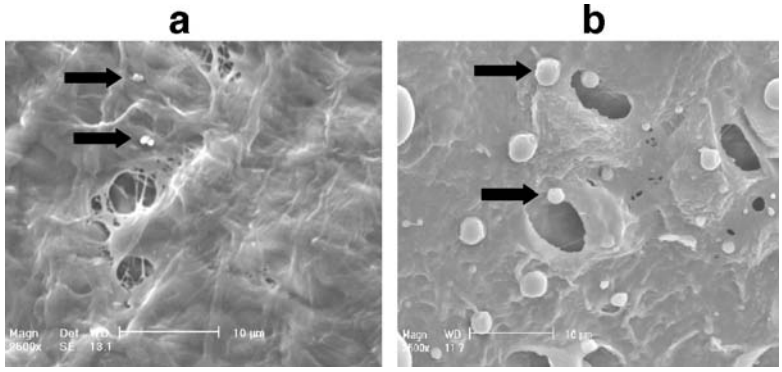

Fig. 4. SEM of openings and particles on diaphragm surface. **a** Nanoparticles (*arrows*). **b** Microparticles (*arrows*). Note that Cremophor micelles (13 nm, not indicated) would be approximately one-fiftieth the size of the nanoparticles.

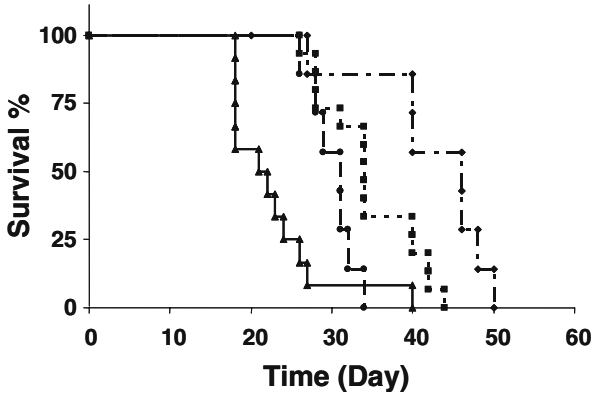

Fig. 5. Effects of carrier on antitumor activity of IP paclitaxel treatments. Mice were implanted 20×10^6 Hs766T tumor cells intraperitoneally. Ten days later, mice were treated with a single IP injection. *From left to right*, physiologic saline (control, n=12, *filled triangle*), paclitaxel nanoparticles (n=7, *filled circle*), paclitaxel in Cremophor EL/ethanol (n=15, *filled square*), and paclitaxel microparticles (n=8, ♦). The paclitaxel-equivalent dose in drug-treated groups was 40 mg/kg. The corresponding median survival times were 22, 34, 31 and 46 days.

Comparison of Particle Size and Lymphatic Duct Openings on Diaphragm Surface

Figure 4 shows the SEM results on the lymphatic duct openings (stomas) on a mouse subdiaphragm surface. We analyzed a total of 175 openings from six mice; the length ranged from 0.7 to 15.5 μm (median, 3.1 μm; mean ± SD, 3.6±2.0 μm) and the width ranged from 0.5 to 8.2 μm (median, 2.1 μm; mean ± SD, 2.4±1.4 μm). The length-to-width ratio ranged from 1 to 2.8 (median, 1.5, mean ± SD, 1.6±0.4). Note the nanoparticles and microparticles located near the openings; the nanoparticles were substantially smaller compared to the openings, whereas the microparticles approached the size of the openings.

Effects of Carrier on Antitumor Activity of Paclitaxel Formulations

Figure 5 shows the results. The untreated control group showed a MST of 22 days. IP treatment with the three formulations significantly prolonged the MST, in the rank order of microparticles (110% increase in MST compared to the control group) > Cremophor formulation (60% increase) > nanoparticles (40% increase). The survival extension in the microparticle group is significantly greater compared to the other two groups (p<0.01, log-rank test).

DISCUSSION

The present study was designed to examine the effects of drug carrier on the disposition and activity of IP therapy, in mice. Results of the whole body autoradiography study provided information on the spatial distribution after intravenous and IP doses of paclitaxel. An IP dose of paclitaxel yielded higher drug concentrations and longer drug retention in the peritoneal cavity and intraperitoneal tissues compared to an intravenous dose of the same formulation, thus confirming the intended peritoneal targeting by IP therapy.

A comparison of the kinetics of the radioactivity in the liver and intestines after the two treatment routes provided some insights on the potential causes of the dose-limiting abdominal/gastrointestinal toxicity of IP paclitaxel. After an intravenous injection, paclitaxel enters the liver where it is metabolized, and the unchanged drug and metabolites undergo biliary excretion into the intestinal lumen (37). In this case, the concentrations in the liver would appear or peak before the concentrations in the intestines, as was observed. After an IP dose, paclitaxel can enter the intestines either directly or indirectly. The indirect path involves being absorbed into systemic circulation followed by liver-to-intestine transfer as for the intravenous administration, in which case paclitaxel would appear first in liver and then in intestines. In the contrary, direct absorption into the intestines would result in the drug appearing first in the intestines, which was the observation of the present study. Such direct absorption has been observed for small and large molecules (e.g., phenol red, insulin) applied to the external serosal surface of the intestinal wall (38,39). Direct absorption into the intestines would bypass the metabolic inactivation in the liver, and would cause the drug to be dispersed in a small volume of fluid in the intestinal tissues/lumen as opposed to the indirect absorption where the drug is dispersed in the much larger volume of plasma or total body water. These IP administration-related changes in drug absorption, distribution and metabolism would expose intestinal tissues to higher concentrations of the unchanged drug and cause greater gastrointestinal toxicity, relative to intravenous paclitaxel.

An earlier study showed that the choice of carrier can affect the toxicity without affecting the antitumor activity of IP paclitaxel in mice; a liposomal formulation was better tolerated by both healthy and tumor-bearing mice (40). Whether the lower toxicity was due to alterations in drug disposition was not studied. The present study used three paclitaxel formulations with different drug release rates and different particle sizes to establish the effects of carrier on the disposition and antitumor activity of paclitaxel. For drug release, the rank order was nanoparticles (100% release in 4 h under sink conditions) > Cremophor formulation (maintaining an equilibrium of about 10% free drug fraction until the entire drug load is released or until depletion of Cremophor micelles) > microparticles (about 70% in 24 h under sink conditions). For particle size, the rank order was microparticles (about 4 μm diameter) > nanoparticles (about 600 nm) > Cremophor micelles (13 nm; (32). These results demonstrate that carrier significantly affected the residence time of paclitaxel in the peritoneal cavity, rate and extent of drug absorption from the cavity into systemic circulation, peritoneal targeting advantage, and survival advantage of the IP treatment.

The present study provided two sets of data that enabled the analysis of the effects of physicochemical properties of drug carriers on the key processes that determine the peritoneal targeting advantage. The plasma concentration-time profiles provided estimates of the effects of drug release from carriers on systemic absorption. The plasma profiles were the net results of three kinetic processes, i.e., drug release from carriers, absorption and metabolism of the free drug by first-pass organs such as the liver (see the kinetic model shown in Fig. 3a). In comparison, the total drug concentration-time profiles in the peritoneal cavity were not

confounded by metabolism and therefore provided more definitive information on the effects of drug release rate and carrier size on the clearance from the peritoneal cavity. These results are discussed as follows.

With respect to the clearance of total drug (sum of free and carrier-bound drug) from the peritoneal cavity, because the clearance of the free paclitaxel will remain the same irrespective of the carrier, the differences observed for the three formulations are due to differences in (a) clearance of the drug-containing carrier and (b) drug release. For drug-containing carriers, because their relatively large size limits the transport through the peritoneum, the major clearance mechanism would be the drainage through the lymphatics. As shown in Fig. 4, the size of the microparticles approaches the micron-size diameter of the openings of the lymphatic ducts, which would limit the lymphatic clearance. In comparison, the smaller, nanosize Cremophor and nanoparticle formulations are readily drained into the lymphatics. Within the nanosize particles, the slower drug release from Cremophor micelles resulted in longer retention of the total paclitaxel (free plus carrier-bound) in the peritoneal cavity, relative to the nanoparticles that had about 50-times larger diameter. This finding, in view of the difference in the free drug fractions in the two formulations (>90% after 3 h for nanoparticles and ~10% for Cremophor micelles), suggests that drug release from carrier as the rate-limiting step for the total paclitaxel to exit the peritoneal cavity. Consistent with this finding, the plasma data showed that microparticles, which had the slowest drug release, yielded the lowest rate and extent of systemic absorption in the first 24 h. In comparison, the two formulations that released the drug load more rapidly (Cremophor and nanoparticle formulations) showed more rapid systemic absorption.

The overall result of the lower systemic absorption and higher peritoneal retention of the microparticles was the 12- to 46-times greater peritoneal targeting advantage and about 2-times longer survival extension in IP tumor-bearing animals, compared to the Cremophor and nanoparticle formulations ($p<0.01$).

To date, there is no chemotherapeutic product specifically designed or approved for IP treatments. IP chemotherapy in patients typically uses the formulations developed for intravenous use. Our results indicate the important roles of drug carrier or formulation in determining the peritoneal targeting advantage and antitumor activity of an IP treatment. The recently completed phase I trial of a polymeric paclitaxel formulation (Paclimer®, 53 μm diameter) revealed the presence of inflammatory cells and polymer filaments in tissues located in the lower part of the abdominal cavity (26), suggesting the localization of microparticles in this area. Further efforts to define the effects of drug carrier properties (e.g., size, surface charge) on intra-abdominal distribution, peritoneal retention and tumor-targeted delivery, as well as studies to evaluate the drug absorption into intestinal tissues and the pharmacodynamic relationship between drug concentration and intestinal toxicity during IP therapy are warranted. Finally, the complex and intertwining kinetic processes that govern the drug release and removal from the peritoneal cavity, as shown in Fig. 3a, suggest the additional need of engineering or computational approaches to make use of the experimental data, in order to arrive at rationally designed drug-loaded carriers that provide the maximal peritoneal targeting while eliminating the need of frequent treatments and local toxicity, in order to optimize IP therapy.

ACKNOWLEDGEMENTS

This work was supported in part by a research grant R37CA49816 and R43CA103133 from the National Cancer Institute, NIH, DHHS.

REFERENCES

1. M. Markman, E. Rowinsky, T. Hakes, B. Reichman, W. Jones, J. L. Lewis, Jr., S. Rubin, J. Curtin, R. Barakat, M. Phillips, and Phase I trial of intraperitoneal taxol: a Gynecoloic Oncology Group study. *J. Clin. Oncol.* **10**(9):1485–1491 (1992).
2. J. L. Speyer, J. M. Collins, R. L. Dedrick, M. F. Brennan, A. R. Buckpitt, H. Londer, V. T. DeVita, Jr., and C. E. Myers. Phase I and pharmacological studies of 5-fluorouracil administered intraperitoneally. *Cancer Res.* **40**(3):567–572 (1980).
3. S. Zimm, S. M. Cleary, W. E. Lucas, R. J. Weiss, M. Markman, P. A. Andrews, M. A. Schiefer, S. Kim, C. Horton, and S. B. Howell. Phase I/pharmacokinetic study of intraperitoneal cisplatin and etoposide. *Cancer Res.* **47**(6):1712–1716 (1987).
4. D. S. Alberts, P. Y. Liu, E. V. Hannigan, R. O'Toole, S. D. Williams, J. A. Young, E. W. Franklin, D. L. Clarke-Pearson, V. K. Malviya, and B. DuBeshter. Intraperitoneal cisplatin plus intravenous cyclophosphamide versus intravenous cisplatin plus intravenous cyclophosphamide for stage III ovarian cancer. *N. Engl. J. Med.* **335**(26):1950–1955 (1996).
5. D. K. Armstrong, B. Bundy, L. Wenzel, H. Q. Huang, R. Baergen, S. Lele, L. J. Copeland, J. L. Walker, and R. A. Burger. Intraperitoneal cisplatin and paclitaxel in ovarian cancer. *N. Engl. J. Med.* **354**(1):34–43 (2006).
6. A. Gadducci, F. Carnino, S. Chiara, I. Brunetti, L. Tanganelli, A. Romanini, M. Bruzzone, and P. F. Conte. Intraperitoneal versus intravenous cisplatin in combination with intravenous cyclophosphamide and epidoxorubicin in optimally cytoreduced advanced epithelial ovarian cancer: a randomized trial of the Gruppo Oncologico Nord-Ovest. *Gynecol. Oncol.* **76**(2):157–162 (2000).
7. M. Markman, B. N. Bundy, D. S. Alberts, J. M. Fowler, D. L. Clark-Pearson, L. F. Carson, S. Wadler, and J. Sickel. Phase III trial of standard-dose intravenous cisplatin plus paclitaxel versus moderately high-dose carboplatin followed by intravenous paclitaxel and intraperitoneal cisplatin in small-volume stage III ovarian carcinoma: an intergroup study of the Gynecologic Oncology Group, Southwestern Oncology Group, and Eastern Cooperative Oncology Group. *J. Clin. Oncol.* **19**(4):1001–1007 (2001).
8. A. Polyzos, N. Tsavaris, C. Kosmas, L. Giannikos, M. Katsikas, N. Kalahanis, G. Karatzas, K. Christodoulou, K. Giannakopoulos, D. Stamatiadis, and N. Katsilambros. A comparative study of intraperitoneal carboplatin versus intravenous carboplatin with intravenous cyclophosphamide in both arms as initial chemotherapy for stage III ovarian cancer. *Oncology* **56**(4):291–296 (1999).
9. J. L. Walker, D. K. Armstrong, H. Q. Huang, J. Fowler, K. Webster, R. A. Burger, and D. Clarke-Pearson. Intraperitoneal catheter outcomes in a phase III trial of intravenous versus intraperitoneal chemotherapy in optimal stage III ovarian and primary peritoneal cancer: a Gynecologic Oncology Group Study. *Gynecol. Oncol.* **100**(1):27–32 (2006).
10. M. S. Yen, C. M. Juang, C. R. Lai, G. C. Chao, H. T. Ng, and C. C. Yuan. Intraperitoneal cisplatin-based chemotherapy vs. intravenous cisplatin-based chemotherapy for stage III optimally cytoreduced epithelial ovarian cancer. *Int. J. Gynaecol. Obstet.* **72**(1):55–60 (2001).
11. E. de Bree, P. A. Theodoropoulos, H. Rosing, J. Michalakis, J. Romanos, J. H. Beijnen, and D. D. Tsiftsis. Treatment of ovarian cancer using intraperitoneal chemotherapy with taxanes:

from laboratory bench to bedside. *Cancer Treat. Rev.* **32**(6):471–482 (2006).
12. http://www.cancer.gov/newscenter/pressreleases/IPchemotherapyrelease.
13. K. B. Goldberg. Phase III Trial shows benefit for old drug, device, for ovarian cancer; will practice change? *Cancer Lett.* **32**(2):1–4 (2006).
14. V. K. Malviya, G. Deppe, G. Boike, and J. Young. Pharmacokinetics of intraperitoneal doxorubicin in combination with systemic cyclophosphamide and cis-platinum in the treatment of stage III ovarian cancer. *Gynecol. Oncol.* **36**(2):185–188 (1990).
15. P. J. O'Dwyer, F. LaCreta, M. Hogan, N. Rosenblum, J. L. O'Dwyer, and R. L. Comis. Pharmacologic study of etoposide and cisplatin by the intraperitoneal route. *J. Clin. Pharmacol.* **31**(3):253–258 (1991).
16. H. Gelderblom, J. Verweij, D. M. van Zomeren, D. Buijs, L. Ouwens, K. Nooter, G. Stoter, and A. Sparreboom. Influence of Cremophor El on the bioavailability of intraperitoneal paclitaxel. *Clin. Cancer Res.* **8**(4):1237–1241 (2002).
17. K. Yokogawa, M. Jin, N. Furui, M. Yamazaki, H. Yoshihara, M. Nomura, H. Furukawa, J. Ishizaki, S. Fushida, K. Miwa, and K. Miyamoto. Disposition kinetics of taxanes after intraperitoneal administration in rats and influence of surfactant vehicles. *J. Pharm. Pharmacol.* **56**(5):629–634 (2004).
18. I. Knemeyer, M. G. Wientjes, and J. L. Au. Cremophor reduces paclitaxel penetration into bladder wall during intravesical treatment. *Cancer Chemother. Pharmacol.* **44**(3):241–248 (1999).
19. W. J. Gradishar, S. Tjulandin, N. Davidson, H. Shaw, N. Desai, P. Bhar, M. Hawkins, and J. O'Shaughnessy. Phase III trial of nanoparticle albumin-bound paclitaxel compared with polyethylated castor oil-based paclitaxel in women with breast cancer. *J. Clin. Oncol.* **23**(31):7794–7803 (2005).
20. M. Harries, P. Ellis, and P. Harper. Nanoparticle albumin-bound paclitaxel for metastatic breast cancer. *J. Clin. Oncol.* **23**(31):7768–7771 (2005).
21. A. Sparreboom, C. D. Scripture, V. Trieu, P. J. Williams, T. De, A. Yang, B. Beals, W. D. Figg, M. Hawkins, and N. Desai. Comparative preclinical and clinical pharmacokinetics of a cremophor-free, nanoparticle albumin-bound paclitaxel (ABI-007) and paclitaxel formulated in Cremophor (Taxol). *Clin. Cancer Res.* **11**(11):4136–4143 (2005).
22. T. K. Yeh, Z. Lu, M. G. Wientjes, and J. L. Au. Formulating paclitaxel in nanoparticles alters its disposition. *Pharm. Res.* **22**(6):867–874 (2005).
23. G. J. Fetterly and R. M. Straubinger. Pharmacokinetics of paclitaxel-containing liposomes in rats. *AAPS PharmSci.* **5**(4):E32 (2003).
24. S. Natsugoe, K. Tokuda, M. Shimada, T. Kumanohoso, M. Baba, S. Takao, M. Tabata, K. Nakamura, H. Yoshizawa, and T. Aikou. Morphology of the designed biodegradable cisplatin microsphere. *Anticancer Res.* **19**(6B):5163–5167 (1999).
25. A. Hagiwara, T. Takahashi, K. Sawai, C. Sakakura, H. Tsujimoto, T. Imanishi, M. Ohgaki, J. Yamazaki, S. Muranishi, A. Yamamoto, and T. Fujita. Pharmacological effects of 5-fluorouracil microspheres on peritoneal carcinomatosis in animals. *Br. J. Cancer* **74**(9):1392–1396 (1996).
26. D. K. Armstrong, G. F. Fleming, M. Markman, and H. H. Bailey. A phase I trial of intraperitoneal sustained-release paclitaxel microspheres (Paclimer) in recurrent ovarian cancer: a Gynecologic Oncology Group study. *Gynecol. Oncol.* **103**(2):391–396 (2006).
27. L. Gianni, C. M. Kearns, A. Giani, G. Capri, L. Vigano, A. Lacatelli, G. Bonadonna, and M. J. Egorin. Nonlinear pharmacokinetics and metabolism of paclitaxel and its pharmacokinetic/pharmacodynamic relationships in humans. *J. Clin. Oncol.* **13**(1):180–190 (1995).
28. C. M. Kearns. Pharmacokinetics of the taxanes. *Pharmacotherapy* **17**(5 Pt 2):105S–109S (1997).
29. Z. Lu, T. K. Yeh, M. Tsai, J. L. Au, and M. G. Wientjes. Paclitaxel-loaded gelatin nanoparticles for intravesical bladder cancer therapy. *Clin. Cancer Res.* **10**(22):7677–7684 (2004).
30. S. Ullberg and B. Larsson. Whole-body autoradiography. *Methods Enzymol.* **77**:64–80 (1981).
31. D. Song and J. L. Au. Isocratic high-performance liquid chromatographic assay of taxol in biological fluids and tissues using automated column switching. *J. Chromatogr. B Biomed. Appl.* **663**(2):337–344 (1995).
32. D. Chen, D. Song, M. G. Wientjes, and J. L. Au. Effect of dimethyl sulfoxide on bladder tissue penetration of intravesical paclitaxel. *Clin. Cancer Res.* **9**(1):363–369 (2003).
33. M. A. Baron. Structure of the intestinal peritoneum in man. *Am. J. Anat.* **69**(3):439–497 (1941).
34. M. F. Flessner, J. D. Fenstermacher, R. G. Blasberg, and R. L. Dedrick. Peritoneal absorption of macromolecules studied by quantitative autoradiography. *Am. J. Physiol.* **248**(1 Pt 2):H26–H32 (1985).
35. W. J. Shih, J. J. Coupal, and H. L. Chia. Communication between peritoneal cavity and mediastinal lymph nodes demonstrated by Tc-99m albumin nanocolloid intraperitoneal injection. *Proc. Natl. Sci. Counc. Repub. China B* **17**(3):103–105 (1993).
36. K. Hirano and C. A. Hunt. Lymphatic transport of liposome-encapsulated agents: effects of liposome size following intraperitoneal administration. *J. Pharm. Sci.* **74**(9):915–921 (1985).
37. B. Monsarrat, P. Alvinerie, M. Wright, J. Dubois, F. Gueritte-Voegelein, D. Guenard, R. C. Donehower, and E. K. Rowinsky. Hepatic metabolism and biliary excretion of Taxol in rats and humans. *J. Natl. Cancer Inst. Monogr.* **15**:39–46 (1993).
38. K. Nishida, A. Kuma, S. Fumoto, M. Nakashima, H. Sasaki, and J. Nakamura. Absorption characteristics of model compounds from the small intestinal serosal surface and a comparison with other organ surfaces. *J. Pharm. Pharmacol.* **57**(8):1073–1077 (2005).
39. K. Waxman, M. H. Soliman, and K. H. Nguyen. Absorption of insulin in the peritoneal cavity in a diabetic animal model. *Artif. Organs* **17**(11):925–928 (1993).
40. A. Sharma, U. S. Sharma, and R. M. Straubinger. Paclitaxel-liposomes for intracavitary therapy of intraperitoneal P388 leukemia. *Cancer Lett.* **107**(2):265–272 (1996).